5

Ultraviolet, Visible, Near-Infrared Spectrophotometers

CHRIS W. BROWN

Department of Chemistry, University of Rhode Island, Kingston, RI, USA

I. INTRODUCTION

Spectrophotometers for the ultraviolet (UV), visible (VIS), and near-infrared (NIR) regions will be discussed in this chapter. Typically, the UV region is considered to extend from 190 to 350 nm, the visible region from 350 to 800 nm, and the NIR from 800 to 2500 nm. However, considerable latitude can be found in the definitions of these regions; the UV might extend up to 400 nm and the short wavelength NIR (SWNIR) from 600 to 1100 nm. The total wavelength range from 190 to 2500 nm is equivalent to a frequency range of about 10^{15}–10^{14} Hz, or a wavenumber range of 50,500–4000 cm^{-1}. In this discussion, we will specifically define the abscissa in terms of wavelength (λ) in nm, although it should be pointed out that wavenumbers are often used in the NIR.

Absorptions in the UV–VIS regions are due to electronic transitions. Most UV–VIS absorptions by organic molecules are attributed to transitions involving nonbonding (n) electrons or electrons in molecular orbitals found in unsaturated molecules. Generally, the absorptions are due to $n \rightarrow \pi^*$ and $\pi \rightarrow \pi^*$ transitions; thus, molecules with double bonds and especially conjugated double bonds such as aromatic compounds are stronger absorbers. UV–VIS spectra of some typical aromatic molecules are shown in Fig. 1 and spectra of several organic dyes in Fig. 2. Most visible dyes consist of polynuclear aromatic ring systems with low energy transitions in the visible region. All aromatic molecules have UV absorptions in the 200–250 nm region. Most NIR absorptions are due to overtone and combinations of fundamentals normally observed in the mid-IR region. Generally, the NIR bands are at least one order of magnitude weaker than the parent absorptions in the mid-IR. One advantage of the NIR is that the decreases in intensities when compared with the mid-IR bands are not the same for all molecules. For example, water is virtually opaque throughout much of the mid-IR region at most pathlengths, but it is much more transparent in the NIR. Thus, it is often possible to observe NIR spectra of solutes dissolved in water. Spectra of three different organic molecules in the NIR are shown in Fig. 3. The patterns in the longer wavelength regions of 2000–2500 nm form a "fingerprint" similar to that observed in the mid-IR region of 600–1800 cm^{-1}.

A. Beer's Law

Absorbance in any spectral region depends on the Beer–Lambert–Bouguer expression commonly known as Beer's Law:

$$A = abc \tag{1}$$

where A is the absorbance, a is the absorptivity or molar extinction coefficient, b is the pathlength, and c is the concentration of the absorbing substance. Both absorbance and absorptivity are wavelength dependent. Actually, a spectrophotometer does not measure the absorbance

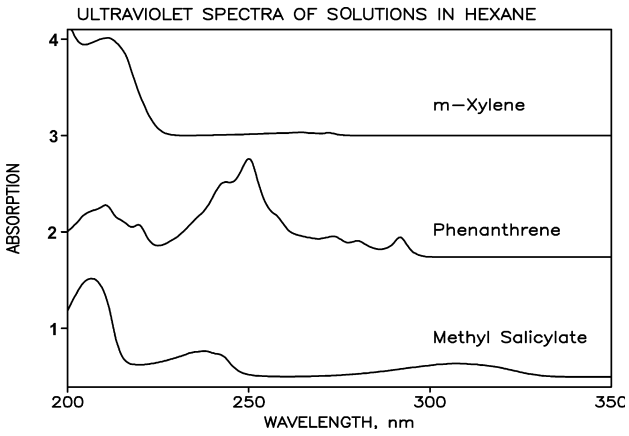

Figure 1 UV spectra of *m*-xylene, phenanthrene, and methyl salicylate.

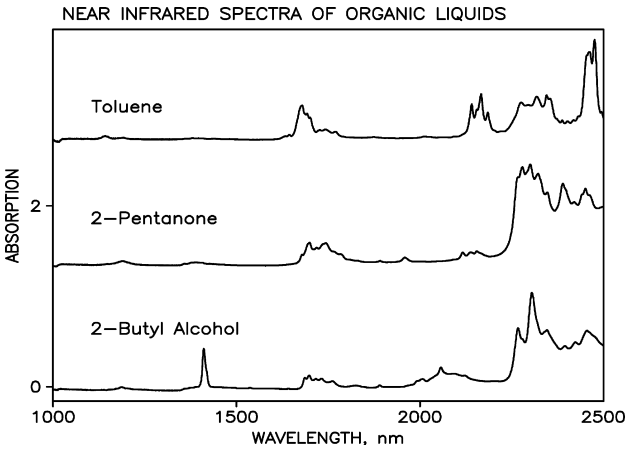

Figure 3 NIR spectra of toluene, 2-pentanone, and 2-butyl alcohol.

directly, but rather it must be calculated by taking the negative logarithm of the fraction of light transmitted through a sample. If P is the power of the light passing through a sample and P_0 is the power of the light detected when the concentration of the absorbing material is zero, the fraction of light transmitted is given by

$$T = \frac{P}{P_0} \tag{2}$$

This is often written as percent transmittance or $\%T$. Absorbance is given by

$$A = -\log T = \log \frac{P_0}{P} \tag{3}$$

The quantities P and P_0 can be measured sequentially on a sample and a blank, or simultaneously with a sample and a blank in two identical cuvets. It is important to keep in mind that A is calculated from T, so that, though noise in the measurements arises in T, its effect on absorbance and concentration is a logarithmic relationship. (The symbol P for the power carried by a light beam is sometimes replaced by I for intensity, but P is the correct term.)

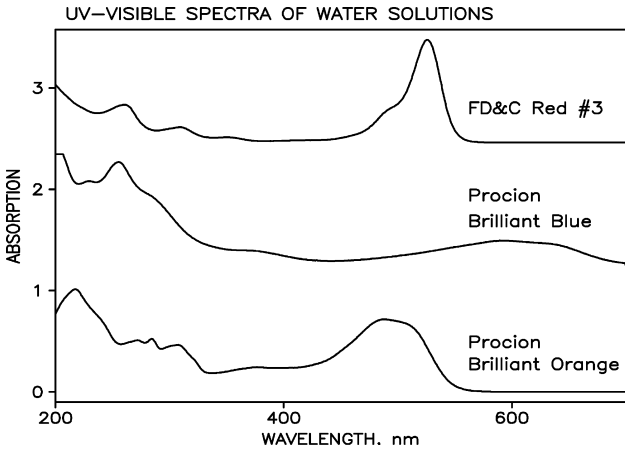

Figure 2 UV–VIS spectra of three dyes.

B. Deviations from Beer's Law

Both chemical and instrumental deviations from Beer's Law may occur. Chemical deviations are caused by reactions such as molecular dissociation or the formation of a new molecule. The most prevalent cause is some type of association due to hydrogen bonding. For example, at very low concentrations in an inert solvent, alcohols exist as monomers but, as the concentration is increased the monomers combine to form dimers, trimers, and so on. Thus, the concentrations and absorbances due to the monomers do not increase linearly with the total concentration of the species. An example of this effect is given in Fig. 4, which shows the NIR spectra of methanol in CCl_4 as a function of concentration. The first overtone of the O—H stretching vibrations of the monomer at 1404 nm does not increase linearly with the total concentration. Moreover, as the total concentration increases, bands due to dimers and oligomers start to appear at slightly longer wavelengths (1450–1650 nm).

There are two primary instrumental deviations from Beer's Law. The first has to do with the fact that the law was defined for monochromatic radiation. Should a sample have entirely different absorptivities at two wavelengths, both falling on the detector at the same time, Eq. (3) would have to be rewritten as

$$A = \log\left(\frac{P_0' + P_0''}{P_0' 10^{-a'bc} + P_0'' 10^{-a''bc}}\right) \tag{4}$$

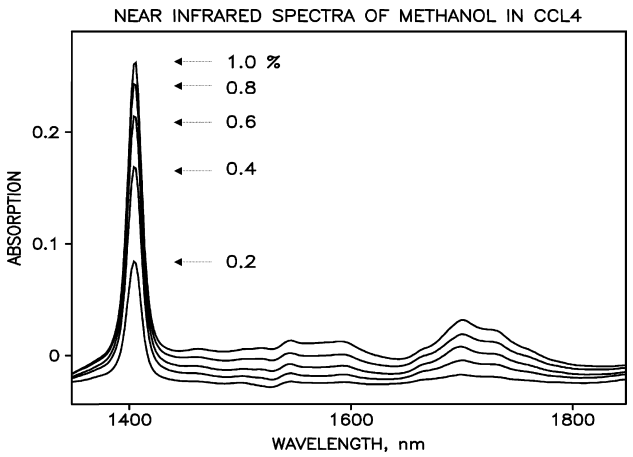

Figure 4 NIR spectra of methanol in CCl_4 as a function of concentration.

where the single and double primes refer to the two wavelengths. Should a' be identical to a'', Eq. (4) reverts to Eq. (3); however, nonlinearity can occur at higher concentrations if there is a significant difference between a' and a''.

The second source of instrumental error is stray light. This problem can be inherent in the spectrometer, but it can also be caused by the operator. Stray light is any light reaching the detector without passing through the sample. Thus, if a sample were completely opaque at a certain wavelength, any photons that were detected would be due to stray light. These photons could be passing around the sample, through holes in the sample as might be caused by air bubbles in a liquid, or they might be the result of poor shielding, permitting room light to reach the detector from some external light source, for example, room lights. The effect of stray light is to add a constant power (intensity) of light, P_s, to both the numerator and denominator in the absorbance expression:

$$A = \log\left(\frac{P_0 + P_s}{P + P_s}\right) \tag{5}$$

As the concentration increases, P approaches zero, and A asymptotically approaches a maximum level given by $\log[(P_0 + P_s)/P_s]$. For P_s equal to 10% of P_0, the maximum value of A is 1.04. As this is a log relation, A approaches 1.04 asymptotically with the concentration. Thus, stray light should be suspected any time when nonlinear data is encountered.

Stray light in a spectrophotometer can be measured by inserting an opaque blocking filter into the optical path. A signal observed by the detector under these conditions is due solely to stray radiation. A 10 g/L solution of potassium iodide does not transmit appreciably below 259 nm, but is essentially completely transparent above 290 nm when observed in a 10 mm cuvet (Poulson, 1964). If a spectrophotometer is set at a lower wavelength, say 240 nm, any signal that is observed must originate from stray radiation. In determining the stray light below 259 nm, the cuvet holding the solution should be placed in the spectrophotometer and scanned from the longer wavelength, transparent region to the shorter, opaque region. In this way the detector signal will be gradually decreased to its lowest level. False readings can sometimes be obtained by inserting a cuvet containing the sample in the spectrophotometer at an opaque wavelength, as the abrupt decrease in signal may not register correctly. In addition, there are other more elaborate procedures given in the literature (Kaye, 1981; 1983) for measuring stray light.

II. SPECTROPHOTOMETER CHARACTERISTICS

The components of a spectrophotometer depend on the region of the electromagnetic spectrum. Historically, a specific region of the spectrum has been defined by the availability of components, sources, and detectors for that region. This is especially true of the UV region in which transmission optics must be made of very pure silica, reflection optics must have a special coating, the source is generally a deuterium lamp, and the detector must be UV-enhanced. In fact, the cross-over from the visible to the UV occurs at about 350 nm, where the visible tungsten-halogen lamp stops emitting and the deuterium lamp is required. At very short wavelengths, ultrapure silica is needed for adequate transmission.

Ideally, a UV–VIS–NIR monochromator should be able to produce either a light beam of nearly monochromatic radiation at the exit slits, or focus nearly monochromatic radiation on individual pixels of an array detector for any wavelength in the range from 190 to 2500 nm. The sensitivity in any part of the region depends on the light source, the composition of the optical components, and the response of the detector. The sensitivity should be such that accurate measurements of transmission can be made from nearly 100% to as low as 0.01% corresponding to between 0 and 4 absorbance units (AU).

The limits of detection are determined by the signal-to-noise (S/N) ratio. At low absorbances (or high transmission), the values of P and P_0 are nearly equal to that their ratio may be lost in the instrument noise. The noise at that level is primarily due to Johnson (thermal) noise in the input resistors and shot noise from detectors, especially, photomultipliers (PMTs) and electrical component connections. At high absorbances (low levels of transmission), the principle source of noise is stray light. In single monochromators with conventional diffraction

gratings, stray light is typically about 0.1% of the total radiant energy at the detector. This can be reduced to about 0.001% by passing the light twice through the grating by modulating the optical beam, or by using a double monochromator. Stray light can be further decreased through the use of holographic gratings to about 0.0005%.

It is necessary to distinguish between slit-width and bandwidth. The term "slit width" refers to the physical separation (in mm) between the slit jaws, whereas "bandwidth" denotes the range of wavelengths passed through the physical slit. For a grating spectrometer, the bandwidth at any wavelength setting is determined by the angular dispersion of the grating and the width of the entrance and exit slits. This is demonstrated for a Czerny–Turner monochromator in Fig. 5. White light enters the entrance slit in the upper left of the figure. The light rays are collimated by a concave mirror so that parallel rays fall on the grating. The light dispersed by the grating is then focused by the second mirror (top right of figure) onto the exit slits. As shown in the figure, the white light is separated into three different wavelengths. Two of these, λ_1 and λ_3, fall on the slit jaws and do not reach the detector, whereas λ_2 falls on the slit opening and then onto the detector. The linear dispersion D (in mm/nm) is given by the relation

$$D = \frac{dy}{d\lambda} = F\frac{dr}{d\lambda} \tag{6}$$

where $dy/d\lambda$ is the wavelength derivative of linear distance across the exit slit, F is the focal length, and $dr/d\lambda$ is the wavelength derivative of the angle of dispersion (the angle between the normal to the grating and the diffracted rays for a particular wavelength). For a given angle of incidence, the angular dispersion of a grating can be expressed as

$$\frac{dr}{d\lambda} = \frac{n}{d\cos r} \tag{7}$$

where n is the order of the grating and d is the distance between grooves. At small angles of dispersion, the cos r approximates unity and

$$D = \frac{nF}{d} \tag{8}$$

Thus, at small angles the linear dispersion of a grating monochromator is a constant, which depends upon the focal length of the monochromator, the distance between the grating grooves, and the grating order.

The resolving power of a monochromator is given as

$$R = \frac{\lambda}{\Delta\lambda} \tag{9}$$

This represents the ability of a monochromator to distinguish between images having slightly different wavelengths. It can be shown (Skoog et al., 1998) that the resolving power is equal to the grating order times the number of grooves across the face of the grating. Thus, the resolving power increases with the order and the physical width of the grating.

The "*f*-number" of a grating monochromator is defined as the focal length divided by the diameter of the collimating mirror. The light gathering power of the monochromator increases as the inverse square of the *f*-number. Thus, an $f/2$ monochromator gathers light $4\times$ as much as an $f/4$ monochromator.

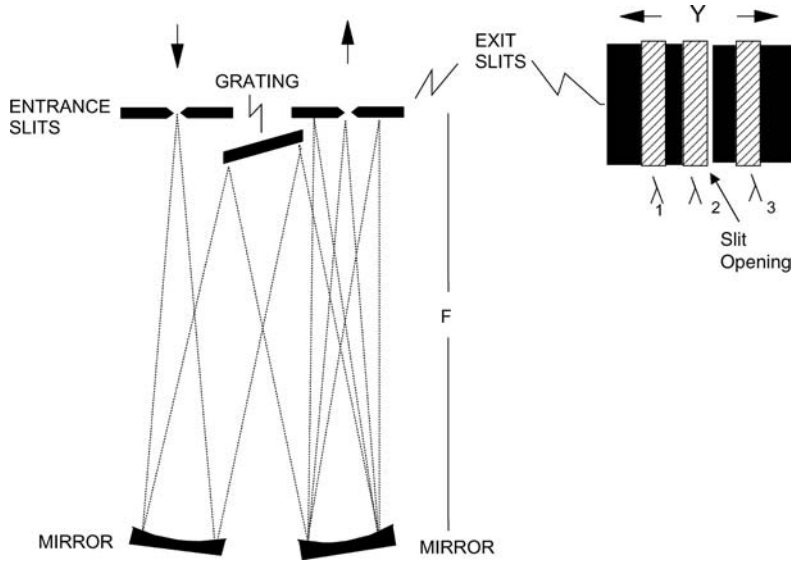

Figure 5 Optical diagram of a Czerny–Turner grating monochromator showing dispersion of light across the exit slits.

A. The Architecture of a Spectrophotometer

There are four basic parts to a spectrophotometer. The source provides radiation over the wavelength range of interest. White light from the source is passed through a wavelength selector that provides a limited band of wavelengths. The radiation exiting the wavelength selector is focused onto a detector which converts the radiation into electrical signals. Finally, the selected signal is amplified and processed as either an analog or a digital signal. We will consider each of the four major components separately.

1. Sources

A deuterium lamp is the primary source of UV radiation. An electric discharge passing through the gas excites the deuterium atoms which then lose their excess energy as the characteristic radiation. High-pressure gas-filled arc lamps containing argon, xenon, or mercury can be used to provide a particularly intense source for specific UV regions. Tungsten-halogen lamps, such as those intended for use in 35 mm projectors, are used for the visible and NIR regions.

2. Wavelength Selectors

The most commonly used wavelength selectors for UV–VIS–NIR spectrophotometers are grating monochromators. However, filter instruments, interferometers, and prism monochromators are sometimes used, and will be discussed here.

Filter Photometers

Absorption filters consist of colored glass or dyed gelatin sandwiched between glass plates. Effective bandwidths range from 30 to 250 nm. Narrow bandwidth filters absorb most of the radiant energy striking them, allowing only a small fraction to pass. Thus, the filters may require air cooling to prevent overheating.

Interference filters are more efficient and more expensive. These filters rely on optical interference to pass a narrow band of wavelengths. The filters consist of two parallel transparent plates coated on their insides with semitransparent metallic films. The space between the two films is filled with a dielectric such as calcium fluoride. Light passing through the first film is partially reflected at the second film. In turn, this reflected beam is partially reflected by the first film, producing interference effects. Those wavelengths that are equal to $2t\eta/n$, where t is the distance between plates, η is the refractive index of the dielectric, and n is the order of the filter (an integer 1, 2, etc.), will be in phase. The bandwidth of these filters is about 1.5% of the wavelength at peak transmittance, where they have a maximum transmittance of about 10%.

Prism Monochromators

The use of prism monochromators has decreased significantly in recent years, primarily because of the fact that the spectrum is a nonlinear function of wavelength and the resolution is not as good as with gratings. However, many prism spectrometers are still in use. The easiest design to visualize is the Bunsen monochromator shown in Fig. 6. Light focused onto the entrance slit is collimated by the first lens, and the parallel rays directed to a glass prism. Light passing through the prism is refracted. Shorter wavelengths are refracted more strongly than longer wavelengths (i.e., blue light is bent more than red). The dispersed light is then focused by the second lens onto the exit slits. Different wavelengths can be focused through the exit slit by either moving the exit slits and lens or by rotating the prism.

Grating Monochromators

Diffraction gratings have become much less expensive and of improved quality in recent years. Gratings can be fabricated for either transmission application or reflection application, but the latter is far more common and will be discussed here. Early gratings were made with elaborate and expensive ruling machines which used a diamond point to scribe each groove in the grating face, one at a time. At present, replica gratings are made from a master that was scribed with the ruling engine on a very hard, optically flat, polished surface. The replicas are made

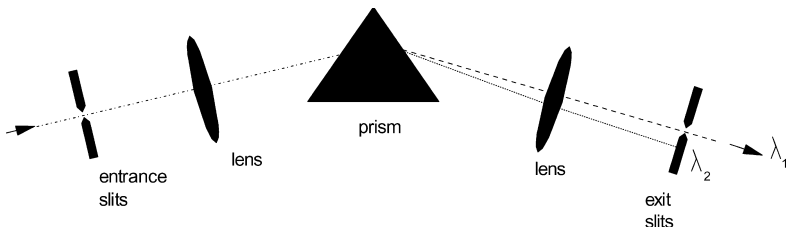

Figure 6 Optical diagram of a Bunsen prism monochromator.

by casting a liquid resin onto the surface of the master. The surface of the replica is made reflecting with a thin coating of aluminum or gold.

Replica gratings are now rapidly being replaced by holographic gratings. These are made using a pair of mutually interfering laser beams to develop a film of photo-resist on a glass surface. The sensitized regions of the photo-resist are etched away leaving a grooved structure that can be coated with a reflective metallic film. The resulting gratings produce more perfect line shapes and provide spectra with reduced stray light, virtually free from the images or ghosts often found in their predecessors.

There are a number of different classic designs for grating monochromators. Probably the most frequently encountered is the Czerny–Turner design shown in Fig. 5. This is a symmetric design with the entrance slit and concave collimating mirror on one side of the normal to the grating and the focusing mirror (identical to the collimating mirror) and exit slit on the other side. The Ebert design shown in Fig. 7(a) is similar, but the two collimating mirrors in the Czerny–Turner design are replaced by a single, large mirror. The Littrow mount shown in Fig. 7(b) is a somewhat more cumbersome, but more compact design. The big advantage of this design is that the size of the monochromator is reduced by using a single mirror to collimate and focus the radiation. Commercial Littrow instruments often place the entrance and exit slits at 90° to each other on the same side of the grating and use a small plane mirror to direct the dispersed light onto the exit slit, as shown in the figure.

Recent emphasis on miniaturization and the increased use of fiber optics have supported the development of miniature spectrophotometers, small enough to fit on a computer card. These monochromators incorporate very small gratings and, in some cases, eliminate the need for mirrors by using a concave grating, which disperses and focuses the light. Exit slits may be used in the focal plane with a single detector, or the slits can be replaced by an array detector for measuring the entire spectrum simultaneously. More will be said about miniature spectrometers and array detectors later.

Interferometers

Michelson interferometers have become the mainstay of mid-IR spectroscopy, to the extent that nearly all grating or prism spectrophotometers for use in the IR have been replaced by Fourier-transform instruments (FTIR), which make use of interferometers. We are now seeing increasing use of interferometers in the NIR region. They have not been as popular in the UV and visible, because the major advantages of the FT approach are not as effective at shorter wavelengths as they are in the mid-IR. The use of interferometers in the NIR warrants a short discussion of their general design.

An optical diagram of the Michelson interferometer is given in Fig. 8. The design is simple and symmetrical.

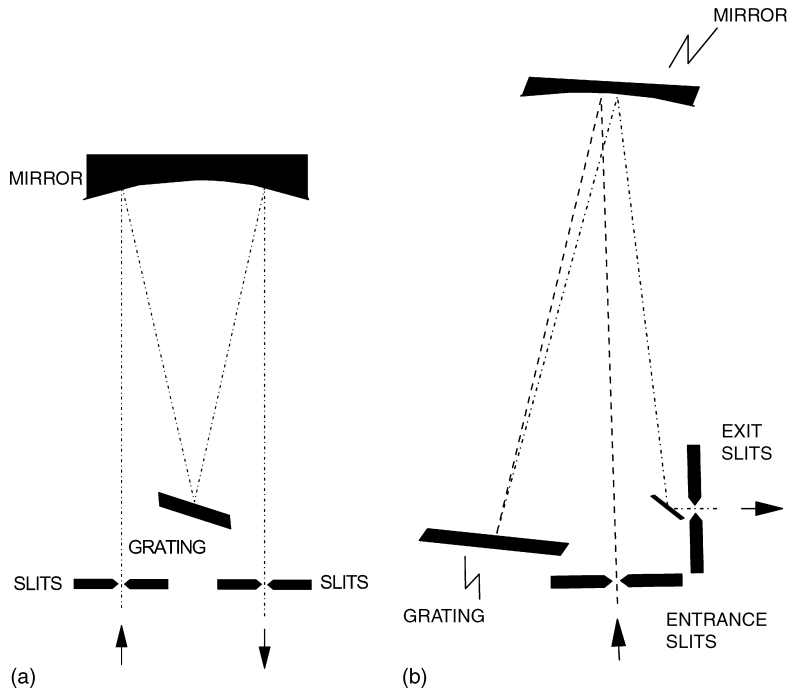

Figure 7 Optical diagram of (a) Ebert grating monochromator and (b) Littrow grating monochromator.

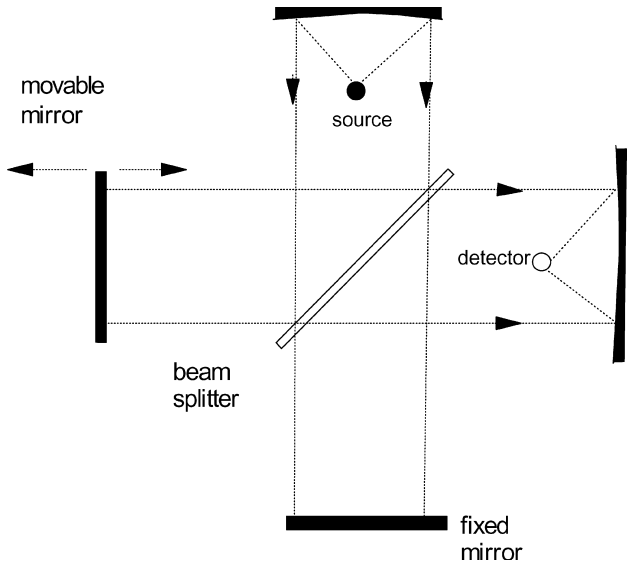

Figure 8 Optical diagram of a Michelson interferometer.

Light rays from a source are collected by a collimating mirror. The collimated rays are split by a beam splitter and directed into the two legs of the interferometer, one half of the light going to a fixed mirror and the other half to a movable mirror. The two reflected beams are recombined at the beam splitter. The phases of the two reflected rays at the beam splitter will depend upon the location of the movable mirror. At any instant in time, some wavelengths will be in-phase and others out-of-phase; the maximum in-phase conditions will occur when the distance of the movable mirror from the beam splitter is exactly equal to the distance of the fixed mirror from the beam splitter. One half of the recombined light will return to the source, and the other half will be transmitted to the detector after passing through the sample. The resulting signal at the detector as a function of the location of the movable mirror is called *interferogram*. The interferogram can be mathematically converted into a spectrum by taking its Fourier transform. Each pass of the movable mirror produces a single interferogram. Successive interferograms can be averaged to improve the S/N ratio.

3. *Detectors*

Certainly, the greatest recent improvements in the spectrophotometers discussed in this chapter have to be in the area of detectors. The mainstay detectors have been phototubes and PMTs; these still have a sizable share of the detector market, but the numerous advances in solid-state detectors have greatly increased their popularity. Improvements and developments in solid-state detectors, especially in the array type, are driven by their use in the consumer market. In the following sections, we will address single and multichannel detectors.

Single-Channel Detectors—Phototubes and PMTs

A vacuum phototube consists of a concave cathode made from (or coated with) a photoemissive material that emits electrons when irradiated with photons. The electrons from the cathode negatively charged by the photons, cross the vacuum to the positive anode and into the amplifier. The number of electrons ejected is directly proportional to the power of the incident radiation. The sensitivity of a photoemissive cathode to various wavelengths depends upon the composition of the emitting surface. For example, a red-sensitive surface is coated with a sequence of metals typically Na/K/Cs/Sb, whereas NIR sensitivity is obtained from coatings made with Ga/In/As. Generally, phototubes have a small dark current resulting from thermally induced electron emission.

PMTs are ideal devices for measuring low-power radiation. In addition to a cathode and an anode, the PMT is provided with a number of other specially shaped electrodes called dynodes. The cathode is the same as that for the photodiode, but is at a much higher negative voltage with respect to ground (e.g., -900 V). The electrons released from the cathode are attracted to the first dynode, which is maintained at a more positive potential (e.g., -810 V) than the cathode. When the electrons from the cathode strike this dynode, they release even more electrons. These electrons are then accelerated to the second dynode, which is at a still more positive potential of -720 V. This multiplication process is repeated over and over until the electrons reach the anode. The collision of each electron with a dynode causes several secondary electrons to be released. In this way, a single photon can produce as many as 10^6–10^7 electrons, with a series of 9 or 10 dynodes. Dark current caused by thermal emission of electrons can be a major problem with PMTs; however, cooling the PMT to -30°C can reduce the thermal causes of dark current to a negligible amount. It should also be mentioned that PMTs are designed for measuring very low levels of light; hence they can be damaged by more intense illumination.

Photovoltaic Detectors

A photovoltaic detector is fundamentally a solid-state DC generator depending on the presence of light to produce a potential. A semiconducting material such as silicon or selenium is deposited as a thin film on a flat piece of steel. The semiconductor is coated with a transparent film of gold or silver to serve as the collector electrode. When radiation of high enough energy reaches the semiconductor, it causes covalent bonds to break producing electrons and holes. The electrons migrate to

the metallic film, and the holes to the steel plate. The electrons produce a current in the external circuit, which is proportional to the radiation. Photovoltaic detectors are used primarily in the visible region, but lack sensitivity at low light levels.

Photodiodes

The photodiode detector consists of a p–n junction diode formed on a silicon chip. A reverse bias is applied to the diode to deplete the electrons and positive holes at the p–n junction as shown in Fig. 9. These are similar to Zener diodes, which pass current when a threshold voltage is reached. In this case, the reverse bias potential is first below the threshold voltage. Photons cause electrons and holes to form in the depletion layer, and these provide a current proportional to the incident radiant power. These devices are more sensitive than phototubes, but less sensitive than PMTs.

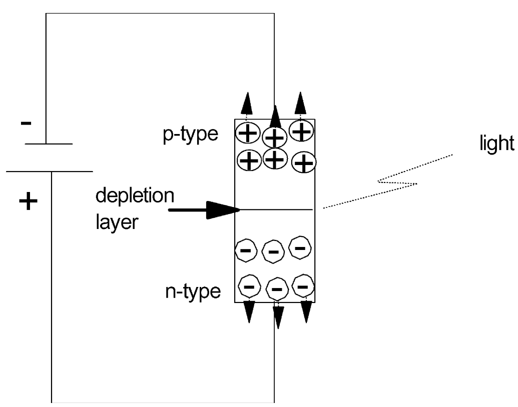

Figure 9 Diagram of a photodiode showing light incident on the depletion layer.

Multichannel Array Detectors

Multichannel detectors consist of 1D or 2D arrays of detector elements. They are all solid-state devices, basically multiple adaptations of the photodiodes discussed earlier. The main advantage of array detectors is speed, as they can measure a complete range of wavelengths simultaneously (Sedlmair et al., 1986).

A 1D array can be made by imbedding small bars of p-type elements in a substrate of n-type silicon on a single chip as shown in Fig. 10. Each p-type element would be connected to a negative potential and the n-type substrate to a positive potential to form the reverse bias. Generally, a 10 μF capacitor is connected in parallel to each p–n pixel. The capacitors are selected sequentially and charged under computer control. Light entering the chip forms electrons and holes at the depletion boundaries of each junction. The amount of current required to recharge the capacitor is proportional to the power of the light falling on that pixel. If this array was used to replace the exit slits of a conventional spectrophotometer, the entrance slit width would be adjusted to match the width of the p-type element, so that the resolution is determined by the size of the p-type elements.

Charge-Transfer Detectors

It is desirable to replace the single-channel PMT tube with a multichannel array for measuring very weak radiations. Attempts have been made to do this with the photodiode arrays, the vidicon tube, and a number of intensified adaptations of these devices, but they do not have sufficient sensitivity, dynamic range, and noise performance to compete with the PMT. These devices, nevertheless, have limited use for multichannel detection where noise and dynamic range are not so important.

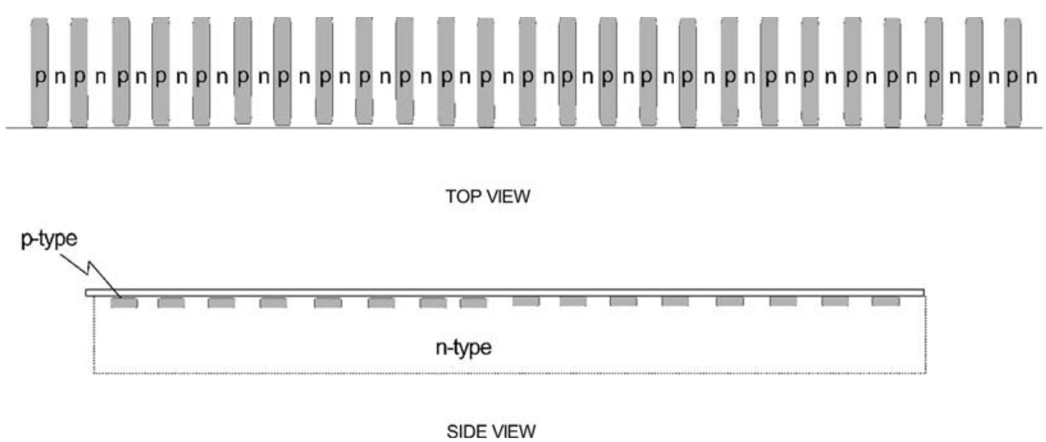

Figure 10 Photodiode array. The top view shows the face that the light would fall upon. The side view shows that the p-type elements are embedded in a continuous layer of n-type material.

Analytical instrumentation has again benefited from developments in the consumer markets. The design and commercialization of video and digital cameras have provided the ideal multichannel array detector for spectroscopic instrumentation. The detectors used in these cameras are a form of charge-transfer detectors (CTD). These detectors (Sweedler et al., 1988) come in two basic types: charge-injection devices (CID) and charge-coupled devices (CCD). Both of these are based on p- and n-doped silicon, but differ in their construction and their methods for handling the charge caused by photons impinging on the surface.

An example of a photon being detected and read from a single-element CID is shown in Fig. 11. Each pixel is connected to two electrodes, one for collecting the charges and one for sensing the total charge. These electrodes are attached across a silica insulator, and each forms a capacitor with the n-doped region. When a photon enters this region, it causes the formation of an electron and a positive hole. The electron goes to the p-doped region and the positive hole is collected near the capacitor formed by the more negative electrode. To read the charge that is built up at this point, the other electrode is disconnected from the applied potential and the voltage (V_1) between it and ground is measured. Next, the voltage on the collector electrode is reversed to positive, which repels all the positive holes. These transfer to the other electrode and are measured as V_2; the difference ($V_2 - V_1$) is proportional to the number of holes, hence to the number of photons. In the last frame of Fig. 11, the charge is removed by making the sensing electrode positive, and the procedure is started all over again.

A diagram of a CCD detector is shown in Fig. 12. For this device, each pixel element consists of a photodiode and a metal-oxide-semiconductor capacitor, which can accumulate and store charge as discussed for the single-element CID. However, the detector/capacitor elements in each row are coupled with the elements in the next lower row. After the charges accumulate in the elements of a row, they are transferred to the next lower row. This transfer is controlled by the parallel clock. Basically, the transfer is performed from the bottom row upward, that is, the bottom is emptied and the charges in the next higher row are transferred downward. Then the charges in the third row are transferred to the second row, and so on. The charges in the elements of the bottom row are transferred to the right side of the sensor array element to element; this transfer is controlled by the serial clock.

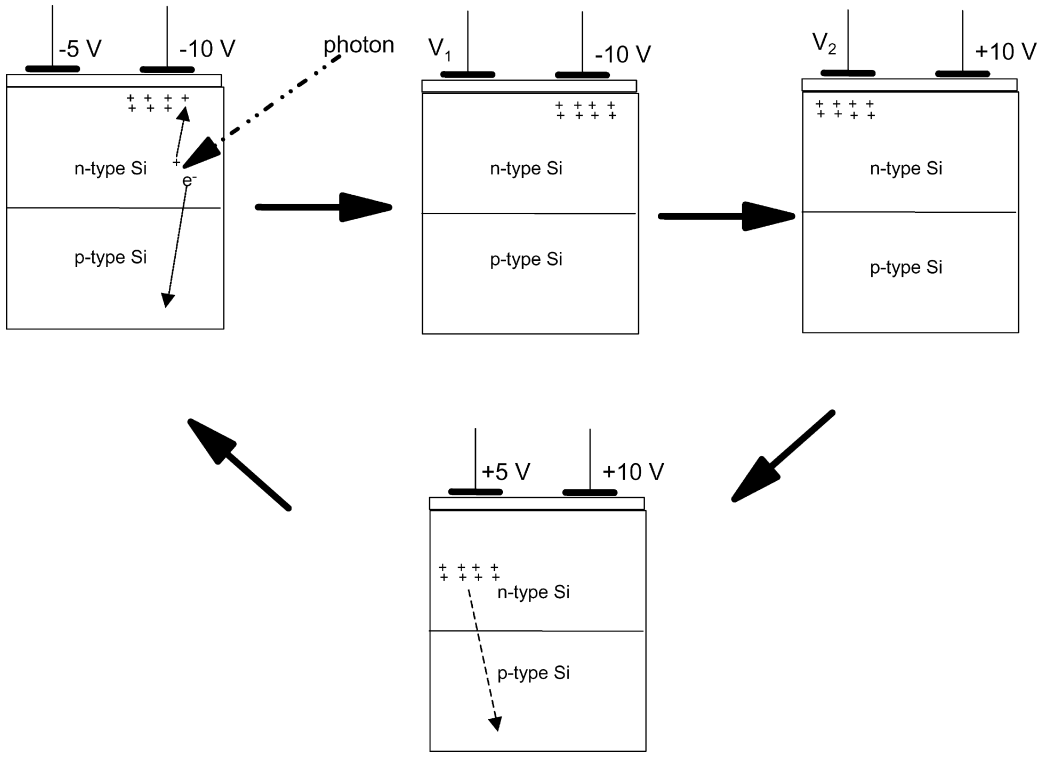

Figure 11 Diagrams showing the effect of a photon falling on a single element in a CID. The photon generates an electron and a positive hole. The measurement is based on counting the number of positive holes accumulated at the more negative electrode. The voltage generated by the positive holes is given by the difference ($V_2 - V_1$), that is, the voltages measured at the left electrode during the second and third frames.

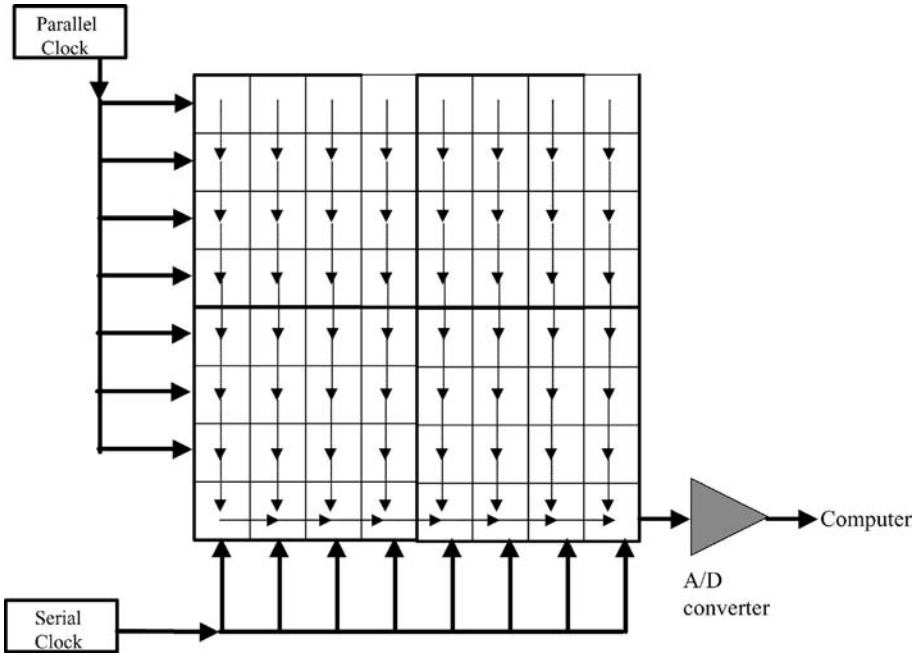

Figure 12 Schematic of a 2D CCD. Each rectangle represents a detector element. The accumulated charges are transferred down the array one row at a time until they reach the registers at the bottom. The charges are transferred serially from left to right across the registers to the A/D converter.

At the right end of the bottom row, the charges are converted to digital signals by an analog-to-digital (A/D) converter. The pixels in a CCD detector have to be read sequentially, whereas those in the CID can be read randomly as each individual element of the CID is connected to an A/D multiplexer.

Basically, the CTDs integrate the charge at each pixel in order to improve the S/N ratio compared with photodiode arrays and vidicons. The CCDs used in video cameras can be incorporated in miniature spectrometers; thus, opening up entirely new uses for analytical instruments.

4. *Signal Processing*

Currently, most spectrophotometers come either with built-in processors or with provision for interfacing to a personal computer. The computer controls the operating settings, adjusts the slits, sets the scan times, and turns on and turns off the light sources. Probably, the more important job for the computer is to acquire and store the spectral data and to convert the data from transmission to absorbance. It may also subtract a background spectrum from the raw data. In addition, the computer may have access to a spectral library for matching an unknown spectrum to a library spectrum, which helps in identification of unknown samples. In any case, it should be possible to display the spectrum on a monitor. It is also possible to smooth the spectrum to reduce the noise, as well as to subtract one spectrum from another, to name a few of the manipulation procedures. Several spectrometer packages provide the user with software for performing multicomponent analyses.

5. *Calibrations*

Some instruments are provided with internal calibration ability, such as testing for photometric accuracy. However, external calibration is often desirable. This is especially true for wavelength calibrations. For complete details on calibrations, the reader should refer to two reviews on the calibration of instruments (Mark, 1992; Mark and Workman, 1992).

Wavelength Calibration

Generally, a glass filter containing didymium or holmium oxide is used for wavelength calibration (Venable and Eckerle, 1979). Both of these can be obtained from the National Institute of Standards and Technology (NIST). Recently, strategies have been described for evaluating wavelength and photometric accuracies, spectral bandwidths, and S/N ratios (Ebel, 1992). Moreover, a wavelength calibration procedure using two well-separated spectral lines has been developed for low-resolution photodiode array spectrophotometers (Brownrig, 1993).

Table 1 Absorptivities in kg/(g cm) of $K_2Cr_2O_7$ in 0.001 M Perchloric Acid at 23.5°C (Brownrig, 1993)

$K_2Cr_2O_7$ (g/kg)	235(1.2)[a] min.	257(0.8) max.	313(0.8) min.	350(0.8) max.	Uncertainty[b]
0.020	12.243	14.248	4.797	10.661	0.034
0.040	12.291	14.308	4.804	10.674	0.022[c]
0.060	12.340	14.369	4.811	10.687	0.020[c]
0.080	12.388	14.430	4.818	10.701	0.020[c]
0.100	12.436	14.491	4.825	10.714	0.019[c]

[a]Wavelength (in nm); spectral bandwidths inside parentheses.
[b]Includes estimated systematic errors and the 95% confidence interval for the mean.
[c]The uncertainty for the 313 nm wavelength is reduced to half for the concentrations marked.

Photometric Accuracy

Solutions of potassium chromate and potassium dichromate have been widely used for checking photometric accuracy. A listing of absorptivities of $K_2Cr_2O_7$ in $HClO_4$ solutions at four wavelengths is given in Table 1 (Mielenz et al., 1977). It should be noted that absorptivities change slightly as a function of concentration. Recently, standard reference materials from NIST for monitoring stability and accuracy of absorbance or transmittance scales have been described (Messman and Smith, 1991). A listing of some standard materials available from NIST is given in Table 2.

6. *Sampling Devices*

Common to most spectrophotometers for the UV–VIS–NIR regions are sampling cuvets with 10.0 mm pathlength. These are available in vitreous silica ("quartz"), UV-transmitting glass, borosilicate glass, and various plastics. Cuvets are also made with pathlengths from 0.1 to 100 mm.

Recent developments in fiber optics technology have greatly enhanced their potential as interfaces between spectrophotometers and samples (Brown et al., 1992). Care must be taken in selecting fibers for the desired optical region. Low-hydroxy silica fibers for the NIR have improved greatly in the past few years, and transmit with very little O–H absorption out to 2000 nm. In the UV region, pure synthetic silica is required, but there is still some loss at the very short wavelengths. In the visible region, silica or glass fibers or even plastic fibers can be used. Fiber optic interfaces are commercially available and a number of instruments are on the market designed for fiber optics, such that the fibers can be fitted directly into the casing of the spectrometer. Although fiber optics offer solutions to many problems, care has to be taken in designing the fiber–sample interface. The cone of light exiting from a fiber can have a relatively large angle and light can be lost, especially if there are changes in refractive index in going from air to sample container to sample. On the whole, fiber optics greatly increases the potential applications for spectroscopic instruments by making it possible to use laboratory instruments for process control and environmental monitoring.

Table 2 NIST Standard Reference Materials for Spectrophotometers (Steward, 1986)

Property tested	Material	Wavelength (nm)
Transmittance	Glass filters	440–635
Absorbance	Liquid filters	302–678
Pathlength	Quartz cuvet	—
UV absorbance	Potassium dichromate	235–350
Fluorescence	Quinine sulfate dehydrate	375–675
Wavelength	Didymium-oxide glass	400–760
Transmittance	Metal-on-quartz filters	250–635
Stray light	Potassium iodide	240–280
Wavelength	Holmium-oxide solution	240–650

III. PRESENT AND FUTURE UV–VIS–NIR SPECTROMETERS

In the early 1970s, UV–VIS–NIR spectrometers were large, stand-alone instruments, which produced a spectrum on a strip-chart recorder. The footprints of the instruments were on the order of several square feet. A spectrum was scanned by moving a grating or a prism and the amplified detector signal was used to move a pen on the strip-chart recorder. By the end of the 1970s, the spectrometers were still the scanning type, but microprocessors and/or computer interfaces had been added to provide spectra in digital format. Array detectors were added to the spectrometers in the 1980s; these eliminated the need for scanning and greatly reduced the time required to obtain a single spectrum. However, the footprints of the instruments were still a few square feet in size.

Two major goals of the developers of chemical and biological instrumentation are miniaturization and spatial image information. These two goals were exemplified by the developments in UV–VIS–NIR instrumentation during the 1990s. By the start of the 21st century, the footprints of many optical spectrometers had been reduced to a few square inches and, in some cases, as small as an integrated circuit chip. Moreover, 2D array type detectors were being used to provide spatial images as a function of wavelength.

Two current, bench top spectrometers, one for the UV–VIS and the other for the NIR region, are shown in Fig. 13. Both of these instruments require a fraction of the space required by their predecessors from the 1980s. Both instruments are interfaced to computers for acquiring, processing, storing, and displaying the spectra. The UV–VIS spectrometer uses diode-array detection, whereas the NIR spectrometer is a rapid-scanning grating instrument.

Miniature spectrometers were marketed in the early 1990s by several companies. The sizes of these spectrometers were on the order of $10 \times 10\,\text{cm}^2$ and could be fitted to a circuit board for plugging directly into a personal computer slot. A popular example of such an instrument is shown in Fig. 14. The footprint of the Ocean Optics package is $\sim 15 \times 15\,\text{cm}^2$, but the actual spectrometer part of the pack is small. The spectrometers can be fitted with several different gratings and CCD array detectors, which are optimized for the spectral region of choice. These spectrometers are designed to be interfaced to samples and sources through a fiber.

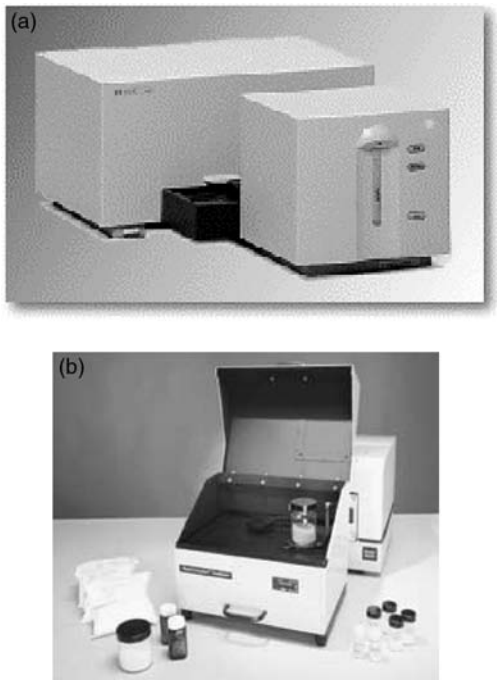

Figure 13 Two 21st Century bench top spectrometers. (a) Agilent Technologies UV–VIS spectrometer with a wavelength range of 190–1100 nm. (b) Foss NIRSystems NIR Rapid Content Sampler with an wavelength range of 1100–2500 nm.

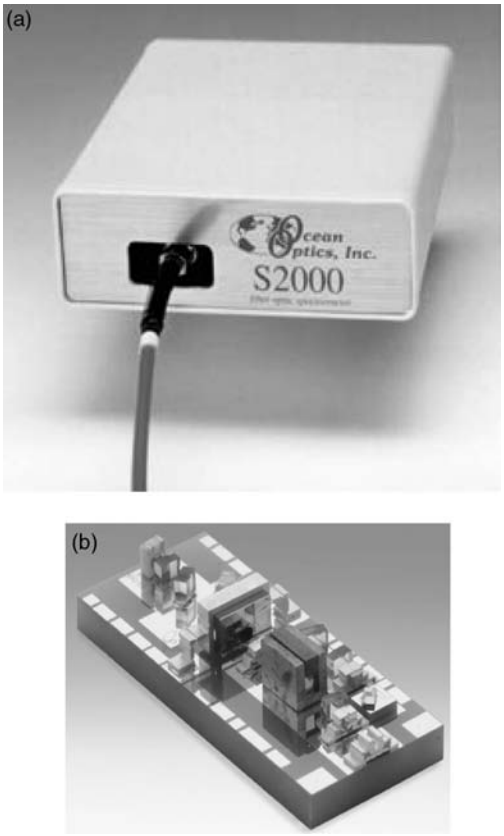

Figure 14 Miniaturized spectrometers. (a) Ocean Optics Model Mode S2000. This spectrometer can be purchased optimized for various spectral regions from 200 to 1100 nm. The miniature spectrometer inside the package is the size of a small circuit board and the footprint of the package is $\sim 15 \times 15\,\text{cm}^2$. (b) AXSUN Technologies microspectrometer showing components on aluminum nitride optical baseplate. The bench is 14 mm long.

The next level of miniaturization of spectrometers has just appeared on the market and is also shown in Fig. 14. All the components of the AXSUN Technologies spectrometer including the source, wavelength selector, and detector are on a chip, which is 14 mm long. This spectrometer is operated in the NIR and is interfaced to a sample by means of a fiber. The wavelength selector is a Fabry–Perot filter, which is simply an interference filter with controllable distances between the parallel reflecting surfaces. The very small size of the Fabry–Perot makes it possible to vary the distance between the reflecting surfaces rapidly, and high-resolution spectra can be acquired in a short time period. This is certainly the first step in the development of microspectrometers, an area that will blossom in the coming years.

Figure 15 Spectral Dimensions Model Sapphire, NIR Chemical Imaging system for measuring NIR microscopic images.

The other important area of 21st century spectroscopy development is in spectral imaging. An example of such a spectrometer for the NIR is shown in Fig. 15. This instrument appears more like a microscope, and it is a microscope that can collect microscopic images over a wavelength range of 1100–2450 nm. An InSb camera with 81,920 pixels (320 × 256 array) is used to measure the spatial image at each wavelength. The wavelength selector for this spectrometer is a liquid crystal tunable filter, which can be rapidly scanned. Imaging spectrometers for the UV–VIS, NIR, and mid-IR came into the market within the last decade. The technology is still very sophisticated and expensive, but major developments have already been made and we will see simpler, less expensive instruments over the next decade.

UV–VIS–NIR spectroscopy will continue to grow and find many uses in this 21st century. More consumer applications of miniature and imaging spectrometers will be found in the medical, transportation, pharmaceutical, and agriculture industries, to name just a few. Technologies developed in laboratories will eventually be used by the layman.

REFERENCES

Brown, C. W., Donahue, S. M., Lo, S-C. (1992). Remote monitoring with near infrared fiber optics. In: Patonay, G., ed. *Advances in Near-IR Measurements*. Vol. 1. JAI Press, p. 1.

Brownrig, J. T. (1993). Wavelength calibration method for low resolution photodiode array spectrometers. *Appl. Spectrosc.* 47:1007.

Ebel, S. F. (1992). *J. Anal. Chem.* 342:1007.

Kaye, W. (1981). Stray light ratio measurements. *Anal. Chem.* 53:2201.

Kaye, W. (1983). *Am. Lab.* 15(1):18.

Mark, H. (1992). *Pract. Spectrosc.* 13:107.

Mark, H., Workman, J. (1992). Statistics in spectroscopy: developing the calibration model. *Spectrosc.* 7:14.

Messman, J. D., Smith, M. V. (1991). *Spectrochim. Acta, Part B* 46B:1653.

Mielenz, K. U., Velapoldi, R. A., Mavrodineanu, R. (1977). *Standardization in Spectrophotometry and Luminescence Measurements*. Special Publication. Washington: National Institute for Standards and Technology, p. 466.

Poulson, R. F. (1964). *Appl. Optics* 3:99.

Sedlmair, J., Ballard, S. G., Mauzrail, D. C. (1986). *Rev. Sci., Instrum.* 57:2995.

Skoog, D. A., Holler, J. F., Nieman, T. A. (1998). *Principles of Instrumental Analysis*. 5th ed. Philadelphia: Harcourt Brace & Company.

Steward, R. W., ed. (1986). *NBS Standard Reference Materials Catalog 1986–87*. Washington: National Institute for Standards and Technology, p. 100.

Sweedler, J. V., Bilhorn, R. B., Epperson, P. M., Sims, C. R., Denton, M. B. (1988). High performance charge transfer device detectors. *Anal. Chem.* 60:282A.

Venable, W. FL., Jr., Eckerle, K. L. (1979). *Didymium Glass Filters for Calibrating the Wavelength Scale of Spectrophotometers*. Special Publication. Washington: National Institute for Standards and Technology, pp. 260–266.